Inorganic Chemistry

pubs.acs.org/IC Article

Construction of Silver Clusters Capped by Zwitterionic Ethynide Ligands

Yang-Lin Shen, Jun-Ling Jin, Jun-Jie Fang, Zheng Liu, Jian-Lin Shi, Yun-Peng Xie,* and Xing Lu*

Cite This: *Inorg. Chem.* 2021, 60, 6276−6282 Read Online

ABSTRACT: A zwitterionic ligand 3-(triethylammonio)propyne (TAP) has been employed to construct nine silver ethynide compounds for the first time. Single-crystal X-ray analyses reveal that compounds **1** and **2** are silver ethynide assemblies based on the Ag_3 subunits and clusters **3**−**8** are small discrete clusters of Ag_3, Ag_6, Ag_8, and Ag_{12}, respectively, ligated by the bulky TAP ligand with different auxiliary ligands. In addition, upon acquiring the tripod-like $^tBuPO_3^{2-}$, a unprecedented 80 nuclei silver ethynide cluster was isolated and determined to be $[(CF_3CO_2)_5@Ag_{80}(TAP)_{14}(^tBuPO_3)_{16}(CF_3CO_2)_{24}]^{19+}$ by crystallography and thermogravimetric analysis. The C_1 symmetry of Ag_{80} was deconstructed to be two $[Ag_{40}(TAP)_7(^tBuPO_3)_8(CF_3CO_2)_{12}]^{12+}$ secondary building subunits arranged in a cross way, with five $CF_3CO_2^-$ trapped in the center. These results highlight that the elaborate selection of ethynide ligands is of great importance in the synthesis of novel silver ethynide clusters.

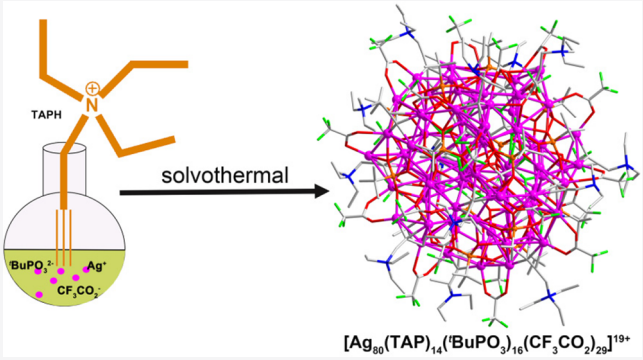

INTRODUCTION

Silver ethynide clusters have attracted great interest due to their fantastic structures and potential applications.[1−8] However, compared with their analogous thiolated silver clusters, the development of silver ethynide clusters has been lagging.[9−13] The easily available thiol ligands with different sizes, structures, and properties promote the booming advancement of thiolated silver clusters.[14−18] Among them, there is a class of zwitterionic thiol ligands for the extensive synthesis of hydrophilic metal clusters,[19,20] while similar zwitterionic ethynide ligands have not yet been explored. The zwitterionic molecule has both cationic and anionic groups[21−23] and possesses an electric dipole moment within the molecule, which has an important impact on the self-assembly process of the cluster.[24] In addition, the charge layer formed by the zwitterionic ligand can effectively passivate the surface of the silver cluster, thereby yielding a small silver cluster.[20,25] Of note, ethynide ligands are known as both σ- and π-donors with silver ions and have various binding motifs.[26,27] Therefore, we envisage that zwitterionic ethynide ligands may provide an opportunity to further stabilize the embryo of silver clusters. Moreover, such small silver ethynide clusters could also be enlarged with help from the bridging ligand phosphonate, which has been repeatedly proven by our group.[28,29]

In this work, we prepared the ethynide ligand TAPH with a one-step reaction according to the reported method[30] and it has been used as protective ligands to assemble nine silver ethynide compounds, which are $\{Ag_3(TAP)(CF_3CO_2)_3\}_n$ (**1**), $\{[Ag_3(TAP)_4]\cdot 3PF_6\}_n$ (**2**), $[Ag_3(TAP)(dppm)_3(CF_3CO_2)]\cdot 2PF_6$ (**3**, dppm = bis(diphenylphosphino)methane), $[Ag_6(TAP)_6(CH_3CN)_6]\cdot 6PF_6$ (**4**), $[Ag_{12}(TAP)_6(CF_3CO_2)_6(CH_3CN)_6(H_2O)_2]\cdot 6PF_6\cdot 6CH_3OH$ (**5**), $[Ag_8(TAP)_8(CH_3CN)_4(H_2O)_2]\cdot 8PF_6\cdot CH_3OH$ (**6**), $[Ag_8(TAP)_6(NO_3)_4(H_2O)_2]\cdot 4PF_6\cdot 2CH_3OH$ (**7**), $[Ag_8(TAP)_6(CF_3CO_2)_4(H_2O)_2]\cdot 4PF_6$ (**8**) and $[Ag_{80}(TAP)_{14}(^tBuPO_3)_{16}(CF_3CO_2)_{29}]\cdot 19PF_6\cdot 177CH_3OH$ (**9**). The zwitterionic ammonium ethynide ligand stabilizes these small ethynide compounds with an interesting external charge layer. Furthermore, $^tBuPO_3^{2-}$ ligands act as a tripodal strut to support the fusion of these small clusters to produce the enlarged cluster Ag_{80}.

RESULTS AND DISCUSSION

X-ray Crystal Structures. X-ray structures of compounds **1**−**9** were determined, and six types of coordination modes for TAP, namely, μ_2-$\eta^1\eta^1$, μ_2-$\eta^1\eta^2$, μ_3-$\eta^1\eta^1\eta^1$, μ_3-$\eta^1\eta^1\eta^2$, μ_4-$\eta^1\eta^1\eta^1\eta^2$, and μ_4-$\eta^1\eta^1\eta^2\eta^2$, occur in these compounds (Figure. 1). Although the coordination modes of TAP and other ethynide ligands are similar, the presence of the bulky

Received: December 30, 2020
Published: April 19, 2021

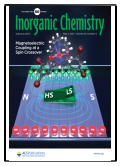

https://doi.org/10.1021/acs.inorgchem.0c03790
Inorg. Chem. 2021, 60, 6276−6282

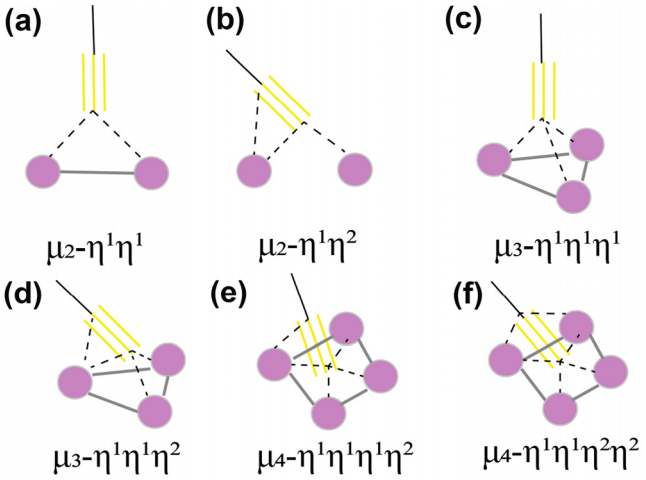

Figure 1. Coordination modes of TAP with silver ions in **1**−**9**. The bulky quaternary N group in TAP is omitted for clarity.

quaternary *N*-group in TAP significantly affects the arrangement of these basic units, dictating the formation of unprecedented structures in **1**−**9**.

Single-crystal X-ray characterization reveals that compound **1** features a polymer-like layered structure composed of $[Ag_3(TAP)(CF_3CO_2)_3]_2$ as structure units. As shown in Figure 2a, $[Ag_3(TAP)(CF_3CO_2)_3]_2$ is yielded by connecting two

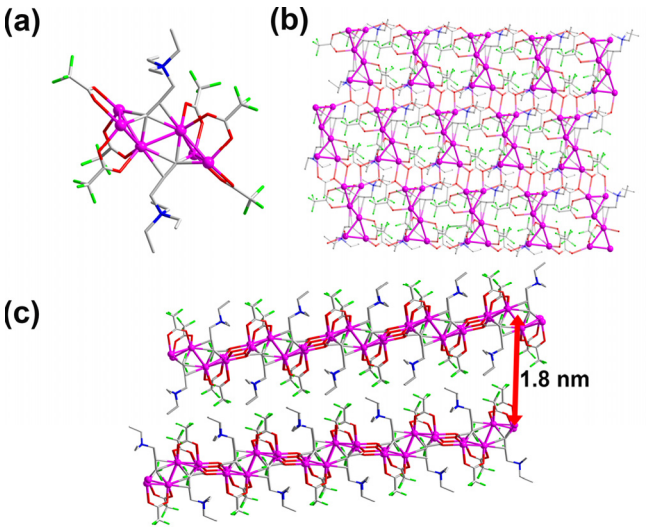

Figure 2. (a) Structure unit of $[Ag_3(TAP)(CF_3CO_2)_3]_2$ and (b and c) the layered structure and spacing of $[Ag_3(TAP)(CF_3CO_2)_3]_n$. Color codes are as follows: Ag, purple; C, gray; N, blue; F, light green; and O, red.

$[Ag_3(CF_3CO_2)_3]$ by two TAP ligands in a mixed σ- and π-type bonding mode (μ_4-$\eta^1\eta^1\eta^1\eta^2$), with Ag−C bond lengths of 2.224−2.626 Å;[31] adjacent Ag_6 units are further connected by carboxylic ligands to form a planar structure with 1.8 nm layer spacing. Interestingly, such a polymer network structure shows that the skeleton is negatively charged, and positively charged quaternary *N*-groups are distributed on both sides of the skeleton,[32,33] which is rarely observed in silver compounds.

The reaction of TAPH·PF_6 with $AgPF_6$ in methanol afforded $\{[Ag_3(TAP)_4]\cdot 3PF_6\}_n$ (**2**). Compound **2** consists of a building block of $[Ag_3(TAP)_4]$ units joined together to form a polymeric chain. The asymmetric Ag_3 unit contains three silver atoms and four TAP ligands, with three PF_6^- serving as counteranions. In detail, the four TAP ligands that exclusively adopt the μ_2-$\eta^1\eta^2$ mode cause one silver atom to be disconnected from the other two silver atoms in the Ag_3 unit (Figure 3). The Ag−C bond lengths in **2** vary from 2.070 to

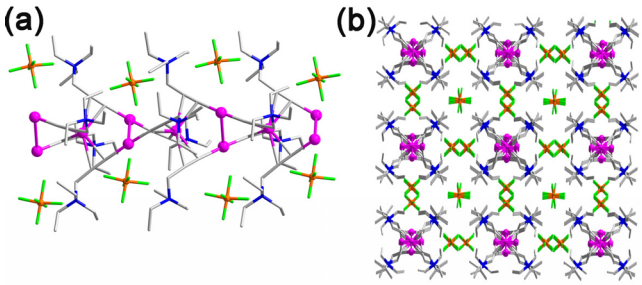

Figure 3. (a) 1D chain structure of $\{[Ag_3(TAP)_4]\cdot 3PF_6\}_n$ (**2**) and (b) the packing structure of **2** viewed along the *c*-axis direction. Color codes are as follows: Ag, purple; C, gray; N, blue; F, light green; P, orange; and O, red.

2.628 Å. The Ag···Ag bond length is 2.936 Å, which is shorter than 3.440 Å and twice the van der Waals radius of silver(I) ion, indicating the presence of argentophilic interactions.[34,35]

Polymeric silver ethynide compounds can be intercepted with auxiliary ligands and often serve as the starting point during the synthesis of discrete clusters. Further investigations revealed that the addition of dppm and acetonitrile gives the formation of the discrete clusters $[Ag_3(TAP)(dppm)_3(CF_3CO_2)]\cdot 2PF_6$ (**3**) and $[Ag_6(TAP)_6(CH_3CN)_6]\cdot 6PF_6$ (**4**), respectively.[36] In **3**, one TAP adopts the μ_3-$\eta^1\eta^1\eta^1$ mode, gripping the Ag_3 unit with bulky dppm ligands that cap the edges. In **4**, six TAP ligands cover the six faces of the Ag_6 octahedron in the μ_3-$\eta^1\eta^1\eta^1$ mode, and each vertex of the octahedron is ligated by an acetonitrile molecule. Besides, the Ag_6 cluster shows a two-layer Ag_3−Ag_3 arrangement, which is consolidated as an integral group by argentophilic interactions (Figure S1). To the best of our knowledge, the discrete Ag_6 octahedral molecule protected by a soft ligand has rarely been prepared.[37−41]

Cluster **5** was prepared by a reaction of TAP and $AgCF_3CO_2$ in a CH_3CN/CH_3OH mixed solvent using the solvothermal method and was identified as $[Ag_{12}(TAP)_6(CF_3CO_2)_6(CH_3CN)_6(H_2O)_2]\cdot 6PF_6\cdot 6CH_3OH$ by crystallography. As shown in Figure 4c, the structure of **5** can be described as the layered structure Ag_3−Ag_3-Ag_3−Ag_3, and there is a similar separation (∼ 2.9 Å) between the adjacent Ag_3 subunits. Besides, the two central and the two outer Ag_3 units are joined by six TAP and six $CF_3CO_2^-$ ligands, where the TAP ligands exclusively adopt the μ_4-$\eta^1\eta^1\eta^1\eta^1$ mode with Ag−C bond lengths ranging from 2.235 to 2.784 Å and each $CF_3CO_2^-$ ligand coordinates with two silver atoms in a μ_2-$\eta^1\eta^1$ mode with Ag−O bond lengths varying from 2.348 to 2.536 Å. Alternatively, as shown in Figure 4d, cluster **5** can also be viewed as a Ag_3−Ag_6−Ag_3 three-layer structure. Considering the same position of TAP ligands in clusters **4** and **5**, cluster **5** is presumably formed via the fusion of **4** and two $[Ag_3(CF_3CO_2)_3]$ units upon a solvothermal reaction. Moreover, the top and bottom surfaces of the Ag_{12} cylinder are covered by auxiliary water molecules. Such a template-free cylinder structure is completely different from

https://doi.org/10.1021/acs.inorgchem.0c03790
Inorg. Chem. 2021, 60, 6276−6282

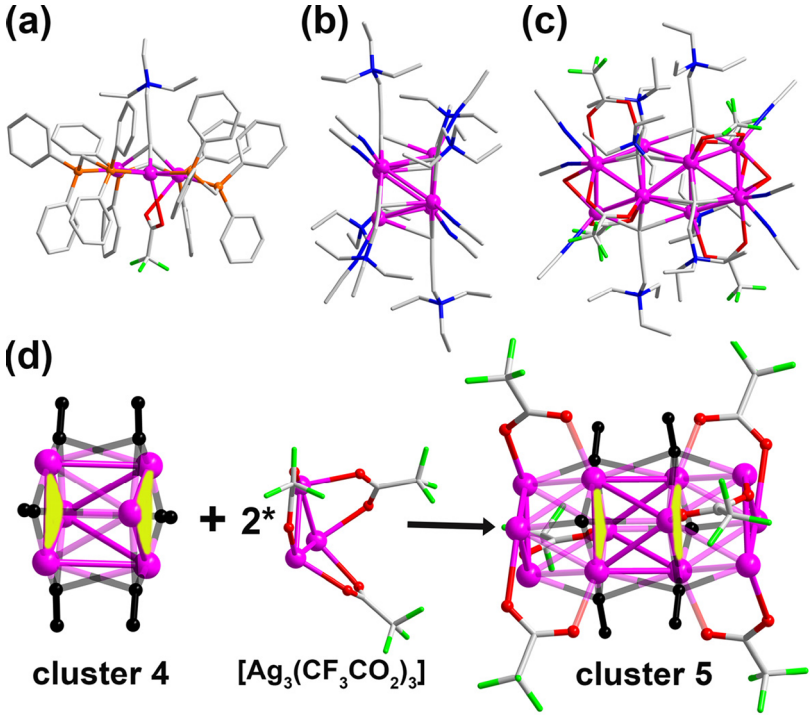

Figure 4. Overview structure of (a) $[Ag_3(TAP)(dppm)_3(CF_3CO_2)]^{2+}$ in **3**, (b) $[Ag_6(TAP)_6(CH_3CN)_6]^{6+}$ in **4**, and (c) $[Ag_{12}(TAP)_6(CF_3CO_2)_6(CH_3CN)_6(H_2O)_2]^{6+}$ in **5**. (d) Generation of cluster **5** from the fusion of **4** and $[Ag_3(CF_3CO_2)_3]$ subunits. Some auxiliary ligands are omitted for clarity. Color codes are as follows: Ag, purple; C, gray, black; N, blue; F, light green; P, orange; and O, red.

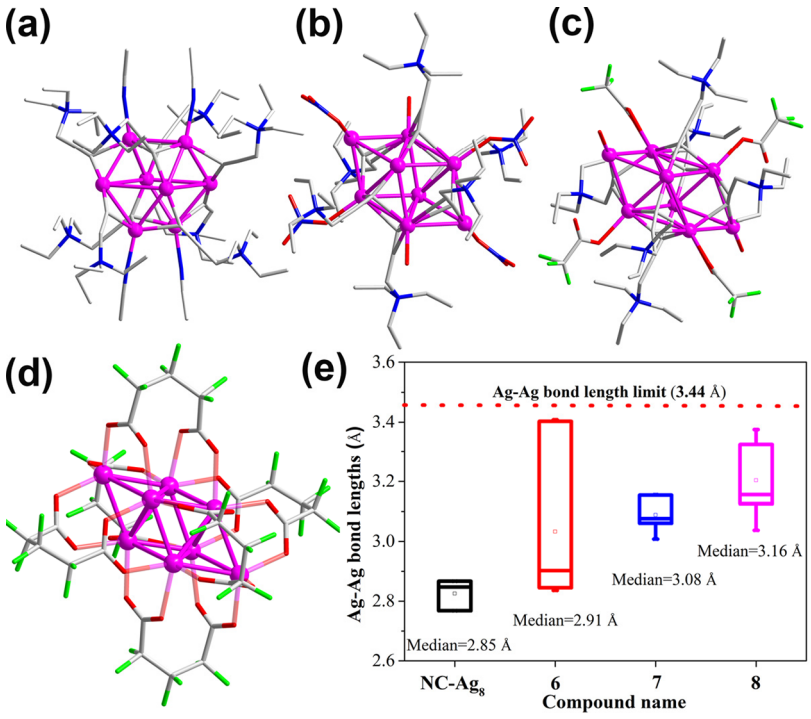

Figure 5. Crystal structure of (a) $[Ag_8(TAP)_8(CH_3CN)_4(H_2O)_2]^{8+}$, (b) $[Ag_8(TAP)_6(NO_3)_4(H_2O)_2]^{4+}$, (c) $[Ag_8(TAP)_6(CF_3CO_2)_4(H_2O)_2]^{4+}$, and (d) $[Ag_8(pfga)_6]^{6-}$ (**NC-Ag$_8$**). (e) The box chart of Ag···Ag bond lengths of the Ag_8 clusters.

the cuboctahedra Ag_{12} synthesized with the *tert*-butylacetylene ligand by Orthaber et al.[31]

The synthesis procedure of **6**−**8** is similar to that of **5** except that different silver salts and solvents were selected in the reaction. According to the single-crystal X-ray analysis, the compounds were determined as $[Ag_8(TAP)_8(CH_3CN)_4(H_2O)_2]\cdot 8PF_6\cdot CH_3OH$ (**6**), $[Ag_8(TAP)_6(NO_3)_4(H_2O)_2]\cdot 4PF_6\cdot 2CH_3OH$ (**7**), and $[Ag_8(TAP)_6(CF_3CO_2)_4(H_2O)_2]\cdot 4PF_6$ (**8**).[42,43,44] As shown in Figure 5, four of the eight TAP ligands in **6** adopt the μ_2-$\eta^1\eta^1$ mode to link two silver atoms, and the remaining four adopt the μ_3-$\eta^1\eta^1\eta^1$ mode to coordinate to three silver atoms, leading

https://doi.org/10.1021/acs.inorgchem.0c03790
Inorg. Chem. 2021, 60, 6276−6282

the eight silver atoms to form an irregular bipyramid with four vertices capped by CH_3CN ligands (Figure S2). In contrast, two TAP ligands in **7** coordinate with silver atoms in the μ_3-$\eta^1\eta^1\eta^1$ mode, and the remaining four TAP ligands use the μ_3-$\eta^1\eta^1\eta^2$ mode to give a novel parallelepiped of Ag_8.[45] Four NO_3^- and two H_2O molecules each coordinate to only one silver atom in the vertices of the parallelepiped. Cluster **8** possesses a similar structure to that of **7** except the four NO_3^- molecules in **7** are replaced by the four $CF_3CO_2^-$ ligands. As shown in Figure 5e, argentophilic interactions are prominent in the formation of clusters **6**−**8** and consolidate their framework as an integral group. It is believed that the attachment of an electron-donating ligand will render silver(I) more electron-rich, resulting in greater charge−charge repulsion and smaller bonding interactions between the silver ions.[46] As expected, NO_3^- anionic ligands in **7** enhance the repulsive force between the silver ions and result in longer Ag···Ag bond lengths than those of **6**, which is coordinated by the electroneutral acetonitrile molecule. While $CF_3CO_2^-$ ligands are bulkier than NO_3^-, they causes cluster **8** to have longer Ag···Ag bond lengths relative to those of **7**. Therefore, we think that both the electron-donating ability and the size of the ligand have a significant influence on argentophilic interactions[47] and further affect the arrangement in these silver cages. Recently, Liu et al. reported the synthesis and structure of the similar parallelepiped-shaped superatomic silver nanocluster $[Ag_8(pfga)_6]^{6-}$ (**NC-Ag$_8$**, pfga = perfluoroglutarate) (Figure 5d).[45] **NC-Ag$_8$** shows the shortest Ag···Ag bond length among these four Ag_8 clusters due to the shell closing of the superatomic orbital ($1S^2$), which presents a sharp contrast with the van der Waals force of the argentophilic interactions in clusters **6**−**8**.

The synthesis of **9** involves a solvothermal reaction where TAPH and the auxiliary ligand $^tBuPO_3H_2$ react with $AgCF_3CO_2$ and triethylamine in methanol. The single-crystal X-ray result displays that cluster **9** crystallizes in the $P2_1/n$ space group. However, the poor crystal quality makes it impossible to model all counterions and solvent molecules, and voids among the crystal structure have been found in the residual electron density in **9** that correspond to 4227 electrons per cell, which were ascribed to 15 PF_6^- counterions and 177 CH_3OH molecules per formula unit.[48] Accordingly, the composition of **9** was determined to be $[Ag_{80}(TAP)_{14}(^tBuPO_3)_{16}(CF_3CO_2)_{29}]\cdot 19PF_6\cdot 177CH_3OH$, and the composition also has been confirmed by the results of XPS and thermogravimetry (Figure S3). The XPS result shows that the silver in the clusters is a +1 valence,[49] and the thermogravimetric curve illustrates a two-step weight loss process that may be caused by a large amount of the crystallization solvent.[21] The total weight loss is similar to the theoretical calculation result.

The skeleton structure of **9** contains 80 Ag ions and 14 TAP, 16 $^tBuPO_3^{2-}$, and 29 $CF_3CO_2^-$ ligands and is identified as a $[Ag_{80}(TAP)_{14}(^tBuPO_3)_{16}(CF_3CO_2)_{25}]^{24+}$ cage, which envelops five asymmetric $CF_3CO_2^-$ molecules. To the best of our knowledge, it is the first time $CF_3CO_2^-$ molecules have been enclosed in silver clusters. These five $CF_3CO_2^-$ ligands evenly occupy the internal space and connect to the wall of the super cage with Ag−F bond lengths that vary from 2.051 to 2.877 Å and Ag−O bond lengths in a range from 2.261 to 2.762 Å.[50] We assume that the hydrothermal conditions and the stable shell formed by $^tBuPO_3^{2-}$ with the silver ions play an important role in enveloping the asymmetric $CF_3CO_2^-$ molecules to form the cluster **9**.

The external skeleton structure of Ag_{80} can be viewed as a construction of two of the same Ag_{40} units. As shown in Figure 6c, Ag_{40} was determined as

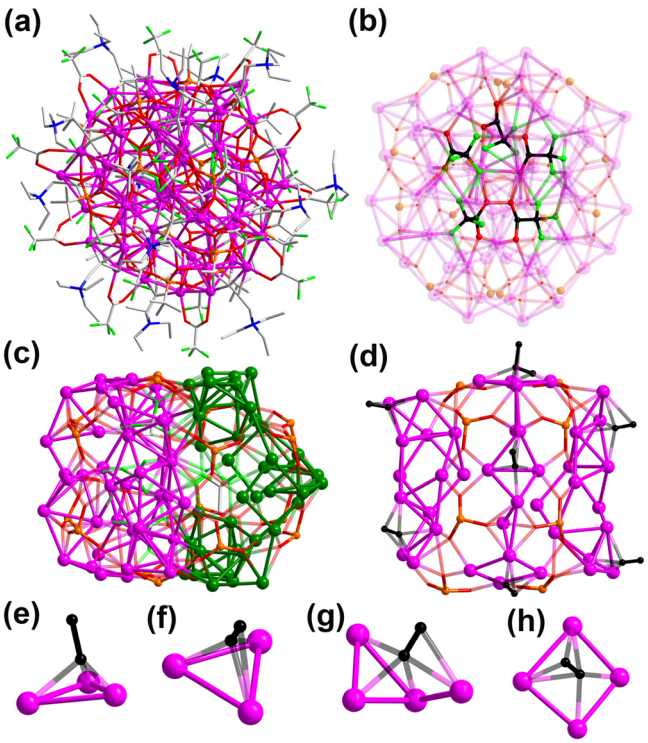

Figure 6. (a) Crystal structure of $[Ag_{80}(TAP)_{14}(^tBuPO_3)_{16}(CF_3CO_2)_{29}]^{19+}$ in **9**. (b) The core−shell structure of Ag_{80}. (c) Relative position of two Ag_{40} units in Ag_{80}. (d) The skeleton structure of $[Ag_{40}(TAP)_7(^tBuPO_3)_8(CF_3CO_2)_{12}]^{12+}$. (e−g) TAP⊃$Ag_3$ and TAP⊃Ag_4 synthons in the shell. Color codes are as follows: Ag, purple, green; C, gray, black; N, blue; F, light green; and O, red. Some alkyl groups are omitted for clarity.

$[Ag_{40}(TAP)_7(^tBuPO_3)_8(CF_3CO_2)_{12}]^{12+}$, which consists of one Ag_{14} and two same Ag_{13} subunits that are located on both sides of the Ag_{14} in a centrosymmetric manner (Figure S4). The Ag_{13} is constructed by synthons of TAP⊃Ag_3 and TAP⊃Ag_4 with six silver ions and five $CF_3CO_2^-$ ligands. In contrast, the Ag_{14} is composed of three TAP⊃Ag_4 synthons with two silver ions and two $CF_3CO_2^-$ ligands. Each of 14 TAP ligands is linked to either three or four silver atoms in the following variant coordination mode: two μ_3-$\eta^1\eta^1\eta^1$, two μ_3-$\eta^1\eta^1\eta^2$, seven μ_4-$\eta^1\eta^1\eta^1\eta^2$, and three μ_4-$\eta^1\eta^1\eta^2\eta^2$ (Figure 6e−h, respectively). Then, these subunits of Ag_{13} and Ag_{14} are connected by the tripodal $^tBuPO_3^{2-}$ ligands in μ_6 or μ_7 modes, with the Ag−O bond length varying from 2.170 to 2.813 Å. Both the Ag_{13} and Ag_{14} are further consolidated by the Ag···Ag interactions with bond lengths ranging from 2.761 to 3.368 Å (Table S2), and there is no significant difference compared to the high-nuclearity silver clusters reported previously (Table S1).[51−53] Considering the similar synthesis conditions of clusters **9** and **5**, the Ag_{13} and Ag_{14} subunits are probably derived from the structural evolution of Ag_{12}. Additionally, eight $^tBuPO_3^{2-}$ ligands join the three subunits together, giving the cambered shape of the Ag_{40} structures. Interestingly, the two Ag_{40} units are combined with the aid of the tripodal

https://doi.org/10.1021/acs.inorgchem.0c03790
Inorg. Chem. 2021, 60, 6276−6282

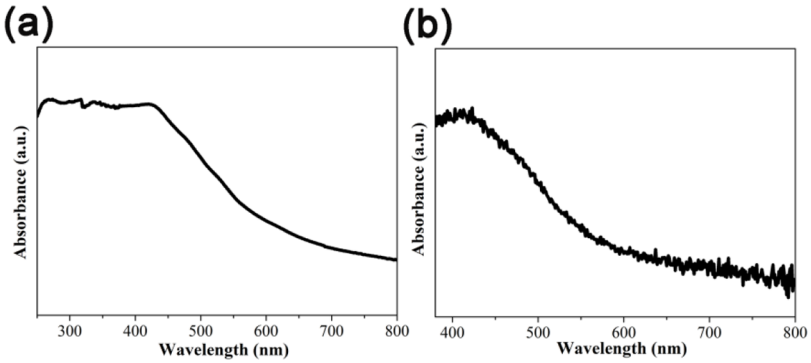

Figure 7. UV−vis absorbance spectrum of **9** in (b) solid and (b) a methanol solution.

^{t}BuPO$_3^{2-}$ligands in a cross way instead of the most common mirror symmetry, which may result from the influence of five inner asymmetric $CF_3CO_2^-$ molecules.

Clusters **1**−**8** have very poor solubilities, but cluster **9** can be dissolved in common organic solvents such as methanol, ethanol, and acetonitrile, which may be due to the large amount of $CF_3CO_2^-$ and ^{t}BuPO$_3^{2-}$ auxiliary ligands in **9**. As shown in Figure 7, the UV−vis spectrum of **9** displays an absorption peak at ca. 410 nm in a methanol solution and shows a wide absorption band ranging from 250 to 550 nm in the solid state, which was assigned to O 2p to Ag 5s charge transfer.[54] Moreover, the fluorescent properties of **9** in solution and the solid state were also explored at room temperature, and no fluorescent emission was observed.[55]

In summary, we synthesized a new ethynide ligand through a simple one-step reaction. Such a zwitterionic ethynide ligand adopts a variety of coordination modes with silver atoms, including μ_2-$\eta^1\eta^1$, μ_2-$\eta^1\eta^2$, μ_3-$\eta^1\eta^1\eta^1$, μ_3-$\eta^1\eta^1\eta^2$, μ_4-$\eta^1\eta^1\eta^1\eta^2$, and μ_4-$\eta^1\eta^1\eta^2\eta^2$. Together with the auxiliary ligands $CF_3CO_2^-$, CH_3CN and dppm to protect the structure edges, two polymeric species and six small silver clusters were prepared. In addition, by introducing a tripod-like ^{t}BuPO$_3^{2-}$, we obtained a rare irregular Ag_{80} structure that encloses five $CF_3CO_2^-$ inside with C_1 symmetry. To our knowledge, this provides the first systematic study of the self-assembly of zwitterion ethynide ligands and silver ions.

■ EXPERIMENTAL SECTION

All reagents and solvents employed are commercially available and were used as received without further purification. Elemental analyses for C, H, and N were performed using a PerkinElmer 2400 CHN elemental analyzer. The Fourier transform infrared (FT-IR) spectra were recorded from KBr pellets in the range 4000−400 cm^{-1} on a Bruker VERTEX 70 spectrometer. The UV-NIR experiments were carried out on a PE Lambda 750S UV−vis-NIR spectrophotometer. Crystal data of **1**−**9** were collected with Mo Kα radiation (λ = 0.71073 Å) on a Bruker D8 Quest diffractometer equipped with a Photon 100 CMOS detector. A multiscan method (SADABS) was used for absorption corrections. The structures were solved by direct methods and refined with SHELXL-2014. Crystallographic data parameters for **1**−**9** are given in Tables S1−S11.

Caution! Silver ethynide complexes are highly potentially explosive in the dry state when subjected to heating or mechanical shock and should be handled in small amounts with extreme care.

Sythesis of TAPH·Br. Propargyl bromide (10 mmol, 0.78 mL) and trimethylamine (12 mmol, 1.7 mL) were mixed in dichloromethane (50 mL) with stirring. After reacting for 30 min, the light yellow precipitate was collected by filtration and washed with diethyl ether. Please pay attention and choose a suitable container to avoid danger due to the violent reaction! Yield: cal 95%. ^{1}H NMR (400 MHz, ACETON-D6, δ, ppm): 1.2−1.3 (t, (C**H**$_3$CH$_2$)$_3$N), 3.3−3.4 (m, (CH$_3$C**H$_2$**)$_3$N), 4.02−4.04 (t, C≡C**H**), 4.31−4.35 (m, NC**H$_2$**C).

Synthesis of TAPH·PF$_6$. TAPH·Br (21.9 g, 0.1 mol) and KPF$_6$ (20.2 g, 0.12 mol) were dissolved in 500 mLof acetonitrile with violent stirring for 48 h. A light yellow solution was collected by filtration and dried with rotary evaporation. Yield: cal 97%.

Synthesis of 1. TAPH·Br (0.03 g, 0.14 mmol) and AgCF$_3$CO$_2$ (0.22 g, 1 mmol) were dissolved in 5 mL of methanol under vigorous stirring at room temperature for 20 min. A clear solution was collected by filtration, and the slow evaporation of the solution afforded the product as colorless crystals. Yield: ca. 25%. IR (KBr, cm^{-1}): 2078 (C≡C), 1681 (C = O), 1133 (C−F). Elemental analysis (%) calcd for $C_{15}H_{17}O_6NF_9Ag_3$: C, 22.47; H, 2.12; N, 1.75. Found: C, 22.56; H. 2.47; N, 1.86.

Synthesis of 2. The synthetic process of **2** is quite similar to that of **1** except that TAPH·Br and AgCF$_3$CO$_2$ were replaced by TAPH·PF$_6$ (0.057 g, 0.20 mmol) and AgPF$_6$ (0.051 g, 0.2 mmol), respectively. Yield: ca. 43%. IR (KBr, cm^{-1}): 2082 (C≡C). Elemental analysis (%) calcd for $C_{36}H_{68}N_4F_{18}P_3Ag_3$: C, 32.87; H, 5.17; N, 4.26. Found: C, 32.98; H, 5.41; N, 4.64.

Synthesis of 3. TAPH·PF$_6$ (0.057 g, 0.20 mmol), dppm (0.153 g, 0.40 mmol), and AgCF$_3$CO$_2$ (0.11 g, 0.5 mmol) were dissolved in 5 mL of methanol under vigorous stirring at room temperature for 20 min. A clear solution was collected by filtration, and the slow evaporation of the solution afforded the product as colorless crystals. Yield: ca. 52%. IR (KBr, cm^{-1}): 2091 (C≡C), 1673 (C=O), 1125 (C−F). Elemental analysis (%) calcd for $C_{86}H_{83}O_2NP_8F_{15}Ag_3$: C, 51.16; H, 4.11; N, 0.69. Found: C, 51.33; H, 4.35; N, 0.83.

Synthesis of 4. TAPH·PF$_6$ (0.057 g, 0.20 mmol) and AgPF$_6$ (0.12 g, 0.5 mmol) were dissolved in 5 mL of acetonitrile. After adding 100 μL of trimethylamine and stirring for 30 min, a clear solution was collected by filtration, and the slow evaporation of the solution afforded the product as colorless crystals. Yield: ca. 34%. IR (KBr, cm^{-1}): 2082 (C≡C). Elemental analysis (%) calcd for $C_{66}H_{120}N_{12}F_{36}P_6Ag_6$: C, 30.50; H, 4.62; N, 6.46. Found: C, 30.72; H, 4.88; N, 6.61.

Synthesis of 5. TAPH·PF$_6$ (0.057 g, 0.20 mmol) and AgCF$_3$CO$_2$ (0.17 g, 0.8 mmol) were dissolved in a mixed solution of methanol (8 mL) and acetonitrile (2 mL). After adding 100 μL of trimethylamine and stirring for 30 min, the mixture was sealed in a 25 mL Teflon-lined stainless steel autoclave and kept at 70 °C for 10 h. The light yellow filtrate was left in dark, giving the product as colorless crystals. IR (KBr, cm^{-1}): 2073 (C≡C), 1677 (C=O), 1116 (C−F). Yield: ca. 19%. Elemental analysis (%) calcd for $C_{84}H_{148}O_{20}N_{12}F_{54}P_6Ag_{12}$: C, 24.30; H, 3.56; N, 4.05. Found: C, 24.42; H, 3.68; N, 4.17.

Synthesis of 6. The synthetic process of **6** is similar to that of **5** except that AgCF$_3$CO$_2$ was replaced with AgPF$_6$ (0.12 g, 0.5 mmol). Yield: ca. 37%. IR (KBr, cm^{-1}): 2132 (C≡C), 839 (P−F). Elemental analysis (%) calcd for $C_{81}H_{152}ON_{12}F_{48}P_8Ag_8$: C, 29.19; H, 4.56; N, 5.04. Found: C, 29.37; H, 4.69; N, 5.16.

Synthesis of 7. The synthetic process of **7** is similar to that of **5** except that AgCF$_3$CO$_2$ was replaced with AgNO$_3$ (0.12 g, 0.5 mmol) and the mixed solvent was replaced with methanol (10 mL). Yield: ca.

https://doi.org/10.1021/acs.inorgchem.0c03790
Inorg. Chem. 2021, 60, 6276−6282

25%. IR (KBr, cm^{-1}): 2069 (C≡C), 1376 (N−O). Elemental analysis (%) calcd for $C_{56}H_{114}O_{16}N_{10}F_{24}P_4Ag_8$: C, 30.50; H, 4.62; N, 6.46. Found: C, 30.72; H, 4.88; N, 6.71.

Synthesis of 8. The synthetic process of **8** is similar to that of **5** except that the amount of $AgCF_3CO_2$ was decreased from 0.8 to 0.5 mmol and the mixed solvent was replaced with methanol (10 mL). Yield: ca. 31%. IR (KBr, cm^{-1}): 2078 (C≡C), 1672 (C = O), 1127 (C−F). Elemental analysis (%) calcd for $C_{62}H_{106}O_{10}N_6F_{36}P_4Ag_8$: C, 26.92; H, 3.83; N, 3.04. Found: C, 27.14; H, 3.97; N, 3.15.

Synthesis of 9. The synthetic process of **9** is quite similar to that of **5** except that the amount of $AgCF_3CO_2$ was increased to 1.3 mmol and $^tBuPO_3H_2$ (0.01 g, 0.1 mmol) was added. Yield: ca. 28%. IR (KBr, cm^{-1}): 2084 (C≡C), 1675 (C=O), 1129 (C−F), 1051 (P=O). Elemental analysis (%) calcd for $C_{425}H_{1084}O_{283}N_{14}F_{201}P_{35}Ag_{80}$: C, 20.87; H, 4.43; N, 0.80. Found: C, 22.61; H, 4.69; N, 1.02.

■ ASSOCIATED CONTENT

Supporting Information

The Supporting Information is available free of charge at https://pubs.acs.org/doi/10.1021/acs.inorgchem.0c03790.

X-ray crystallography data and additional figures (PDF)

Accession Codes

CCDC 2031013−2031021 contain the supplementary crystallographic data for this paper. These data can be obtained free of charge via www.ccdc.cam.ac.uk/data_request/cif, or by emailing data_request@ccdc.cam.ac.uk, or by contacting The Cambridge Crystallographic Data Centre, 12 Union Road, Cambridge CB2 1EZ, UK; fax: +44 1223 336033.

■ AUTHOR INFORMATION

Corresponding Authors

Yun-Peng Xie − *State Key Laboratory of Materials Processing and Die & Mould Technology, School of Materials Science and Engineering, Huazhong University of Science and Technology (HUST), Wuhan 430074, China;* orcid.org/0000-0002-4065-9809; Email: xieyp@hust.edu.cn

Xing Lu − *State Key Laboratory of Materials Processing and Die & Mould Technology, School of Materials Science and Engineering, Huazhong University of Science and Technology (HUST), Wuhan 430074, China;* orcid.org/0000-0003-2741-8733; Email: lux@hust.edu.cn

Authors

Yang-Lin Shen − *State Key Laboratory of Materials Processing and Die & Mould Technology, School of Materials Science and Engineering, Huazhong University of Science and Technology (HUST), Wuhan 430074, China*

Jun-Ling Jin − *Henan Key Laboratory of Functional Salt Materials, Center for Advanced Materials Research, Zhongyuan University of Technology, Zhengzhou 450007, China*

Jun-Jie Fang − *State Key Laboratory of Materials Processing and Die & Mould Technology, School of Materials Science and Engineering, Huazhong University of Science and Technology (HUST), Wuhan 430074, China*

Zheng Liu − *State Key Laboratory of Materials Processing and Die & Mould Technology, School of Materials Science and Engineering, Huazhong University of Science and Technology (HUST), Wuhan 430074, China*

Jian-Lin Shi − *State Key Laboratory of Materials Processing and Die & Mould Technology, School of Materials Science and Engineering, Huazhong University of Science and Technology (HUST), Wuhan 430074, China*

Complete contact information is available at: https://pubs.acs.org/10.1021/acs.inorgchem.0c03790

Notes

The authors declare no competing financial interest.

■ ACKNOWLEDGMENTS

We gratefully acknowledge financial support from the National Natural Science Foundation of China (nos. 21771071, 51672093, and 21925104). We thank the Analytical and Testing Center at the Huazhong University of Science and Technology for all related measurements.

■ REFERENCES

(1) Zhang, X.; Wang, J.-Y.; Huang, Y.-Z.; Yang, M.; Chen, Z.-N. Silver(I) nanoclusters of carbazole-1,8-bis(acetylide): from visible to near-infrared emission. *Chem. Commun.* **2019**, *55*, 6281−6284.

(2) Zhang, S.-S.; Alkan, F.; Su, H.-F.; Aikens, C. M.; Tung, C.-H.; Sun, D. $Ag_{48}(C{\equiv}C^tBu)_{20}(CrO_4)_7$: An atomically precise silver nanocluster co-protected by inorganic and organic ligands. *J. Am. Chem. Soc.* **2019**, *141*, 4460−4467.

(3) Wang, T.; Zhang, W.-H.; Yuan, S.-F.; Guan, Z.-J.; Wang, Q.-M. An alkynyl-protected Au_{40} nanocluster featuring PhC≡C-Au-P^P motifs. *Chem. Commun.* **2018**, *54*, 10367−10370.

(4) Jin, J.-L.; Shen, Y.-L.; Xie, Y.-P.; Lu, X. Silver ethynide clusters constructed with fluorinated *β*-diketonate ligands. *CrystEngComm* **2018**, *20*, 2036−2042.

(5) Shen, H.; Mizuta, T. An atomically precise alkynyl-protected $PtAg_{42}$ superatom nanocluster and its structural implications. *Chem. - Asian J.* **2017**, *12*, 2904−2907.

(6) Wu, H.-B.; Huang, Z.-J.; Wang, Q.-M. Unprecedented solution-stable silver(I) ethynediyl clusters. *Chem. - Eur. J.* **2010**, *16*, 12321−12323.

(7) Xie, Y.-P.; Mak, T. C. W. Silver(I)-ethynide clusters constructed with phosphonate-functionized polyoxovanadates. *J. Am. Chem. Soc.* **2011**, *133*, 3760−3763.

(8) Koshevoy, I. O.; Karttunen, A. J.; Kritchenkou, I. S.; Krupenya, D. V.; Selivanov, S. I.; Melnikov, A. S.; Tunik, S. P.; Haukka, M.; Pakkanen, T. A. Sky-blue luminescent Au^I-Ag^I alkynyl-phosphine clusters. *Inorg. Chem.* **2013**, *52*, 3663−3673.

(9) Xie, Y.-P.; Jin, J.-L.; Duan, G.-X.; Lu, X.; Mak, T. C. W. High-nuclearity silver(I) chalcogenide clusters: A novel class of supramolecular assembly. *Coord. Chem. Rev.* **2017**, *331*, 54−72.

(10) Lei, Z.; Wan, X.-K.; Yuan, S.-F.; Wang, J.-Q.; Wang, Q.-M. Alkynyl-protected gold and gold-silver nanoclusters. *Dalton Trans.* **2017**, *46*, 3427−3434.

(11) Jin, R.; Zeng, C.; Zhou, M.; Chen, Y. Atomically precise colloidal metal nanoclusters and nanoparticles: fundamentals and opportunities. *Chem. Rev.* **2016**, *116*, 10346−10413.

(12) Yang, J.; Jin, R. New advances in atomically precise silver nanoclusters. *ACS Materials Lett.* **2019**, *1*, 482−489.

(13) Hau, S. C. K.; Cheng, P.-S.; Mak, T. C. W. Enlargement of globular silver alkynide cluster *via* core transformation. *J. Am. Chem. Soc.* **2012**, *134*, 2922−2925.

(14) Ren, L.; Yuan, P.; Su, H.; Malola, S.; Lin, S.; Tang, Z.; Teo, B. K.; Hakkinen, H.; Zheng, L.; Zheng, N. Bulky surface ligands promote surface reactivities of $[Ag_{141}X_{12}(S\text{-}Adm)_{40}]^{3+}$ (X = Cl, Br, I) nanoclusters: models for multiple-twinned nanoparticles. *J. Am. Chem. Soc.* **2017**, *139*, 13288−13291.

(15) Desireddy, A.; Conn, B. E.; Guo, J.; Yoon, B.; Barnett, R. N.; Monahan, B. M.; Kirschbaum, K.; Griffith, W. P.; Whetten, R. L.; Landman, U.; Bigioni, T. P. Ultrastable silver nanoparticles. *Nature* **2013**, *501*, 399−402.

(16) Joshi, C. P.; Bootharaju, M. S.; Alhilaly, M. J.; Bakr, O. M. $[Ag_{25}(SR)_{18}]^-$: The "golden" silver nanoparticle. *J. Am. Chem. Soc.* **2015**, *137*, 11578−11581.

(17) Dhayal, R. S.; Lin, Y. R.; Liao, J. H.; Chen, Y. J.; Liu, Y. C.; Chiang, M. H.; Kahlal, S.; Saillard, J. Y.; Liu, C. $[Ag_{20}\{S_2P(OR)_2\}_{12}]$: A superatom complex with a chiral metallic core and high potential for isomerism. *Chem. - Eur. J.* **2016**, *22*, 9943−9947.
(18) Wang, Z.; Su, H.-F.; Tan, Y.-Z.; Schein, S.; Lin, S.-C.; Liu, W.; Wang, S.-A.; Wang, W.-G.; Tung, C.-H.; Sun, D.; Zheng, L.-S. Assembly of silver Trigons into a buckyball-like Ag_{180} nanocage. *Proc. Natl. Acad. Sci. U. S. A.* **2017**, *114*, 12132−12137.
(19) Bao, S.-J.; Liu, C.-Y.; Zhang, M.; Chen, X.-R.; Yu, H.; Li, H.-X.; Braunstein, P.; Lang, J.-P. Metal complexes with the zwitterion 4-(trimethylammonio)benzenethiolate: Synthesis, structures and applications. *Coord. Chem. Rev.* **2019**, *397*, 28−53.
(20) Huo, S.; Jiang, Y.; Gupta, A.; Jiang, Z.; Landis, R. F.; Hou, S.; Liang, X.-J.; Rotello, V. M. Fully zwitterionic nanoparticle antimicrobial agents through tuning of core size and ligand structure. *ACS Nano* **2016**, *10*, 8732−8737.
(21) Li, Z.; Cai, W.; Yang, X.; Zhou, A.; Zhu, Y.; Wang, H.; Zhou, X.; Xiong, K.; Zhang, Q.; Gai, Y. Cationic metal−organic frameworks based on linear zwitterionic ligands for $Cr_2O_7^{2-}$ and ammonia sensing. *Cryst. Growth Des.* **2020**, *20*, 3466−3473.
(22) Blackman, L. D.; Gunatillake, P. A.; Cass, P.; Locock, K. E. S. An introduction to zwitterionic polymer behavior and applications in solution and at surfaces. *Chem. Soc. Rev.* **2019**, *48*, 757−770.
(23) Shao, Q.; Jiang, S. Molecular understanding and design of zwitterionic materials. *Adv. Mater.* **2015**, *27*, 15−26.
(24) Yi, M.; Lau, C. H.; Xiong, S.; Wei, W.; Liao, R.; Shen, L.; Lu, A.; Wang, Y. Zwitterion−Ag complexes that simultaneously enhance biofouling resistance and silver binding capability of thin film composite membranes. *ACS Appl. Mater. Interfaces* **2019**, *11*, 15698−15708.
(25) Gong, T.; Yang, X.; Sui, Q.; Qi, Y.; Xi, F.-G.; Gao, E.-Q. Magnetic and photochromic properties of a manganese(II) metal-zwitterionic coordination polymer. *Inorg. Chem.* **2016**, *55*, 96−103.
(26) Tang, J.; Zhao, L. Polynuclear organometallic clusters: synthesis, structure, and reactivity studies. *Chem. Commun.* **2020**, *56*, 1915−1925.
(27) He, X.; Liu, H.-X.; Zhao, L. Integration of acetylenic carbon clusters and silver clusters: template synthesis and stability enhancement. *Chem. Commun.* **2016**, *52*, 5682−5685.
(28) Xie, Y.-P.; Jin, J.-L.; Lu, X.; Mak, T. C. W. High-nuclearity silver thiolate clusters constructed with phosphonates. *Angew. Chem., Int. Ed.* **2015**, *54*, 15176−15180.
(29) Jin, J.-L.; Xie, Y.-P.; Cui, H.; Duan, G.-X.; Lu, X.; Mak, T. C. Structure-directing role of phosphonate in the synthesis of high-nuclearity silver (I) sulfide-ethynide-thiolate clusters. *Inorg. Chem.* **2017**, *56*, 10412−10417.
(30) Zhao, B.; Gao, Z.; Zheng, Y.; Gao, C. Scalable synthesis of positively charged sequence-defined functional polymers. *J. Am. Chem. Soc.* **2019**, *141*, 4541−4546.
(31) Gupta, A. K.; Orthaber, A. The self-assembly of $[\{Ag_3(C{\equiv}C^tBu)_2\}_n]^{n+}$ building units into a template-free cuboctahedron and anion-encapsulating silver cages. *Inorg. Chem.* **2019**, *58*, 16236−16240.
(32) Aulakh, D.; Varghese, J. R.; Wriedt, M. A new design strategy to access zwitterionic metal−organic frameworks from anionic viologen derivates. *Inorg. Chem.* **2015**, *54*, 1756−1764.
(33) Zhan, N.; Palui, G.; Safi, M.; Ji, X.; Mattoussi, H. Multidentate zwitterionic ligands provide compact and highly biocompatible quantum Dots. *J. Am. Chem. Soc.* **2013**, *135*, 13786−13795.
(34) Schmidbaur, H.; Schier, A. Argentophilic interactions. *Angew. Chem., Int. Ed.* **2015**, *54*, 746−784.
(35) Su, Y. M.; Wang, Z.; Schein, S.; Tung, C. H.; Sun, D. A Keplerian Ag_{90} nest of Platonic and Archimedean polyhedra in different symmetry groups. *Nat. Commun.* **2020**, *11*, 3316−3325.
(36) Jin, J.-L.; Xie, Y.-P.; Lu, X. High-nuclearity silver ethynide clusters containing polynucleating oxygen donor ligands. *Dalton Trans.* **2018**, *47*, 12972−12978.
(37) Wang, Z.; Qu, Q.-P.; Su, H.-F.; Huang, P.; Gupta, R. K.; Liu, Q.-Y.; Tung, C.-H.; Sun, D.; Zheng, L.-S. A novel 58-nuclei silver nanowheel encapsulating a subvalent Ag_6^{4+} kernel. *Sci. China: Chem.* **2020**, *63*, 16−20.
(38) Wang, Z.; Su, H.-F.; Kurmoo, M.; Tung, C.-H.; Sun, D.; Zheng, L.-S. Trapping an octahedral Ag_6 kernel in a seven-fold symmetric Ag_{56} nanowheel. *Nat. Commun.* **2018**, *9*, 2094−2111.
(39) Wang, Z.; Yang, F.-L.; Yang, Y.; Liu, Q.-Y.; Sun, D. Hierarchical multi-shell 66-nuclei silver nanoclusters trapping subvalent Ag_6 kernels. *Chem. Commun.* **2019**, *55*, 10296−10299.
(40) Han, Z.; Dong, X.-Y.; Luo, P.; Li, S.; Wang, Z.-Y.; Zang, S.-Q.; Mak, T. C. W. Ultrastable atomically precise chiral silver clusters with more than 95% quantum efficiency. *Sci. Adv.* **2020**, *6*, No. eaay0107.
(41) Deng, C.; Sun, C.; Wang, Z.; Tao, Y.; Chen, Y.; Lin, J.; Luo, G.; Lin, B.; Sun, D.; Zheng, L. A sodalite-type silver orthophosphate cluster in a globular silver nanocluster. *Angew. Chem., Int. Ed.* **2020**, *59*, 12659−12663.
(42) Wang, Z.; Su, H.-F.; Gong, Y.-W.; Qu, Q.-P.; Bi, Y.-F.; Tung, C.-H.; Sun, D.; Zheng, L.-S. A hierarchically assembled 88-nuclei silver-thiacalix [4] arene nanocluster. *Nat. Commun.* **2020**, *11*, 308−315.
(43) Yuan, P.; Zhang, R.; Selenius, E.; Ruan, P.; Yao, Y.; Zhou, Y.; Malola, S.; Häkkinen, H.; Teo, B. K.; Cao, Y.; Zheng, N. Solvent-mediated assembly of atom-precise gold−silver nanoclusters to semiconducting one-dimensional materials. *Nat. Commun.* **2020**, *11*, 2229−2236.
(44) Kephart, J. A.; Boggiano, A. C.; Kaminsky, W.; Velian, A. Inorganic clusters as metalloligands: Ligand effects on the synthesis and properties of ternary nanopropeller clusters. *Dalton Trans.* **2020**, *49*, 16464−16473.
(45) Liu, K.-G.; Gao, X.-M.; Liu, T.; Hu, M.-L.; Jiang, D.-e. All-carboxylate-protected superatomic silver nanocluster with an unprecedented rhombohedral Ag_8 Core. *J. Am. Chem. Soc.* **2020**, *142*, 16905−16909.
(46) Wing-Wah Yam, V.; Chung-Chin Cheng, E.; Zhu, N. Synthesis, photophysics, and electrochemistry of hexanuclear silver(I) chalcogenolate complexes. X-Ray crystal structures of $[Ag_6(\mu\text{-dppm})_4(\mu_3\text{-}SC_6H_4Me\text{-}p)_4](PF_6)_2$ and $[Ag_6(\mu\text{-dppm})_4(\mu_3\text{-}SeC_6H_4Cl\text{-}p)_4](PF_6)_2$. *New J. Chem.* **2002**, *26*, 279−284.
(47) Shen, Y.-L.; Jin, J.-L.; Xie, Y.-P.; Lu, X. *tert*-Butyl thiol and pyridine ligand co-protected 50-nuclei clusters: the effect of pyridines on Ag−SR bonds. *Dalton Trans.* **2020**, *49*, 12574−12580.
(48) Sheldrick, G. M. Crystal structure refinement with *SHELXL*. *Acta Crystallogr., Sect. C: Struct. Chem.* **2015**, *71*, 3−8.
(49) Wu, T.; Yin, D.; Hu, X.; Yang, B.; Liu, H.; Xie, Y.-P.; Liu, S.-X.; Ma, L.; Gao, G.-G. A disulfur ligand stabilization approach to construct a silver(I)-cluster-based porous framework as a sensitive SERS substrate. *Nanoscale* **2019**, *11*, 16293−16298.
(50) Guan, Z.-J.; Zeng, J.-L.; Yuan, S.-F.; Hu, F.; Lin, Y.-M.; Wang, Q.-M. $Au_{57}Ag_{53}(C{\equiv}CPh)_{40}Br_{12}$: A large nanocluster with C_1 symmetry. *Angew. Chem., Int. Ed.* **2018**, *57*, 5703−5707.
(51) Liu, K.-G.; Chen, S.-K.; Lin, Y.-M.; Wang, Q.-M. An organic anion template: a 24-nucleus silver cluster encapsulating a squarate dimer. *Chem. Commun.* **2015**, *51*, 9896−9898.
(52) Liu, K.-G.; Liu, X.-Y.; Guan, Z.-J.; Shi, K.; Lin, Y.-M.; Wang, Q.-M. The transformation of polyoxometalates in the formation of intercluster compound $[Ag_{41}(\alpha\text{-}SiW10O_{37})(^tBuC{\equiv}C)_{27}(CH_3CN)_3]$-$[\beta\text{-}SiW_{12}O_{40}]$. *Chem. Commun.* **2016**, *52*, 3801−3804.
(53) Qiao, J.; Shi, K.; Wang, Q.-M. A giant silver alkynyl cage with sixty silver(I) ions clustered around polyoxometalate templates. *Angew. Chem., Int. Ed.* **2010**, *49*, 1765−1767.
(54) Liu, K.-G.; Bigdeli, F.; Li, H.-J.; Li, J.-Z.; Yan, X.-W.; Hu, M.-L.; Morsali, A. Hexavalent octahedral template: a neutral high-nucleus silver alkynyl nanocluster emitting infrared light. *Inorg. Chem.* **2020**, *59*, 6684−6688.
(55) Zhang, S.-S.; Su, H.-F.; Wang, Z.; Wang, L.; Zhao, Q.-Q.; Tung, C.-H.; Sun, D.; Zheng, L.-S. Anion-templated nanosized silver alkynyl clusters: cluster engineering and solution behavior. *Chem. - Eur. J.* **2017**, *23*, 3432−3437.